J. Basic. Appl. Sci. Res., 2(5)4939-4951, 2012
© 2012, TextRoad Publication
ISSN 2090-4304
Journal of Basic and Applied Scientific Research
www.textroad.com

Optimization of Electric Field in 230kV Power Transformers Bushing

M. Hassani [*1], H. Hafezinasab [2], S. S. Karimi Madahi [3], Majid Alambeygi[4]

[1] Department of Electrical Engineering, Islamshahr Branch, Islamic Azad University, Islamshahr, Iran
[2] Department of Electrical Engineering, Ashtian Branch, Islamic Azad University, Ashtian, Iran
[3,4] Department of Electrical Engineering, Islamshahr Branch, Islamic Azad University, Islamshahr, Iran

ABSTRACT

Condenser bushings are one of the key components in power transformers. Although their price is negligible compared to the total price of the transformer their quality has an important effect on performance and reliability of the transformer. In high voltage condenser bushing, the intensity of voltage and electric field on bushing abacus is very high. This high intensity is also observed in flange parts. The amount of multi -layer insulator among the electrodes or floating plates in capacitor bushing make equi-potential surfaces and reduction of electric field in these areas can greatly improve the capacitor bushing performance.
In this paper, we investigate the reduction of field intensity and electrical tension and also improvement in voltage control by displacing floating points which are in the form of aluminum foils stick to impregnated paper.
KEYWORDS: Aluminum foil, conceder bushing, electrical discharge, electric field, voltage distribution.

INTRODUCTION

Insulators are among the most important components used in different parts of a power system including substations, transmission and distribution lines. So their performance has a significant effect on power system characteristics. The intensity of voltage and electric field, in addition to creating corona effect on insulator surface, makes partial discharges on existing cavities on the insulator surface. This changes the electrical and mechanical characteristics of insulator and makes it completely damaged. To avoid corona and partial discharges in power transformer bushings, the electric field on bushing and its insulator, using the change in the structure of floating condenser plates, should be controlled.

Many simulations have been done for electric field on a power transformer condenser bushing [1-3]. Today, the floating plate structure is the most important topic in condenser bushings [1, 3-7]. Reduction of electrical tension in porcelain insulators using floating plates structure is one of the major problems in condenser bushings [1, 8-10]. For this purpose, displacement of the lower edge to a lower position relative to the upper edge and bending the corners of foils is done to reduce the electrical tensions.

The changes are effective to make the electric field constant and also to reduce electrical tension over stick condenser layers which are in the metal flange and also over bushing insulator [1]. The study of electric field in high voltage devices using light technology is also very important to investigate the performance of internal and external points of device for the break down voltage and also electric field condition in the vicinity of light [11].

To the best of our knowledge, high voltage bushings are not still simulated by MAXWELL13 software. But investigation of electric fields on bushing and insulators has already been done by FIELD, FEMLAB, FEM, FLUX [1-6].

There is also no report on optimization of electric field on porcelain bushing there are also some studies available in literature for improvement of electric field and voltage distribution in the overlapping section of edges, effect of displacement of aluminum foil in the overlapping section of these edges and effect of foil corner [1]. The corona loop is also effectively used for optimizing and employing the bushing [12]. In the active region in the overlapping edges using displacement aluminum foil edges and also changing the shape of foil edges by displacing the lower edge to a position lower than upper edge improve the electric field and voltage distribution around the edges. On the contrary, displacement of lower edge to a position upper than the upper edge increases the electric field intensity [1]. One of the other important factors on electric field is folding in the corners of foils. Unfolded corners and displacement of the lower foil corner edge to a position lower than upper foil edge is very effective in optimization of electric field intensity [1]. For design and implementation of this type of equipments it is necessary to simulate electric field so that the design fits the optical sensor. The optimum design of dimensions and size and corona loop position which is done in a way to fit the bushing and the electric field around the sensor are used for optimal design of optical sensor. The results of simulation are used in the implementation of the device. The dimensions and suitable corona size and its installation position on bushing to improve the electric field to permissible limits were calculated for silicon shield. The electric field intensity for suitable design of optical sensor was also calculated.

In this paper, we investigate the reduction of field intensity and electrical tension and also improvement in voltage control by displacing floating points which are in the form of aluminum foils stick to impregnated paper.

CONDENSER BUSHING

Condenser bushing is one of the parts of power transformers which is used in input and output terminals to avoid electrical arc between the line and the chassis of transformer. These insulators are in the form of cylindrical layers and depending on where they are used have different shapes, presented in Fig. 1.

***Corresponding Author:** Mahdi Hassani, Department of Electrical Engineering, Islamshahr Branch, Islamic Azad University, Islamshahr, Iran, phone: +98 935 9783057, email: mahdi_hassani1@yahoo.com

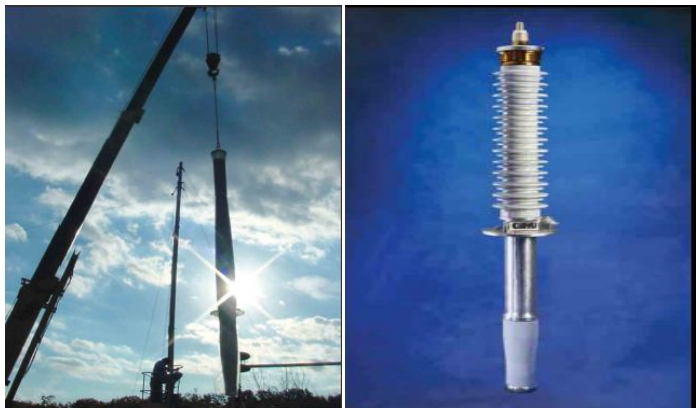

Fig. 1. Condenser bushing

In voltage levels of 72.5 kV and above due to the need to optimized design of dimensions, it is only condenser bushing that is applicable [7,13]. The height of bushings differs according to voltage level and their distance from earth. All high voltage bushing insulators have a creep length of 20kV/cm [7,14].

Bushings, on the basis of their voltage and current, are made in different sizes and the number of abacuses and their length is chosen according to the required voltage. In order to prevent electric discharge in bushings plates, special care must be paid that no edge notching, crack or ragged surface happen [3,6,15-16]. The shape and size of bushings depends on voltage level, their location (indoor or outdoor) and their nominal voltage. Outdoor bushings are completely in the face of weather conditions like snow, rain, pollution, etc so they are different in shape and are made of abacus like buffers. That keeps their lower surface away from rain. Thus their outer surface increases and the arc creep length voltage on the porcelain insulator increases too which makes the electrical strength better [17,18].

THE PROPOSED MODEL FOR ELECTRIC FIELD FUNCTION

The electric field function for any component in an electric network can be attained using Maxwell's equations. Thus the electric field function around a bushing can be written using these equations. For the complexity of structure and arrangement of foils in the structure shown in Fig. 2 the electric field distribution function around the condenser bushing can hardly be described by Maxwell equations thus we try to attain the electric field function around the bushing by a logical analysis.

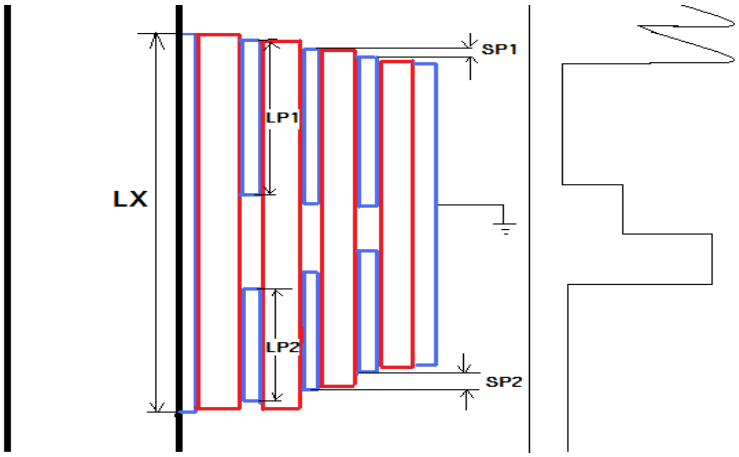

Fig. 2. Complexity of structure and arrangement of foils in bushing structure

In Fig. 2 we have:

L_X - length of the first aluminum foil
Lp_1 - upper aluminum foil length
Lp_2 - lower aluminum foil length
Sp_1 - longitudinal distance between two upper adjacent foils
Sp_2 - longitudinal distance between two lower adjacent foils

Electric field should be a function of electric potential so we have Eq. (1).

$$E=f(V) \quad (1)$$

Electric field is also inversely proportional to the length of foils thus we have Eq. (2).

$$E=f(V/Lx) \quad (2)$$

To change the Eq. (2) from proportionality into equality, it is necessary to multiply or divides, a coefficient like α, by fraction V/Lx which yields Eq. (3).

$$E=V/\alpha Lx \tag{3}$$

Electric field is directly proportional with longitudinal distance between two foils. As the electric field is inversely proportional to the length of aluminum foils and directly proportional to longitudinal distance between two adjacent foils, the electric field function will be like Eq. (4).

$$E=\frac{V}{\alpha L_x(\frac{L_p}{S_p})} \tag{4}$$

Since in the proposed structure there are two sets of aluminum foils (upper and lower), the Eq. (4) is modified to Eq. (5) where there is a coefficient for each aluminum foil.

$$E=\frac{V}{\alpha L_x(\beta\frac{L_{p1}}{S_{p1}}+\gamma\frac{L_{p2}}{S_{p2}})} \tag{5}$$

There is a problem with Eq. (5) which occurs when the longitudinal distance between two adjacent foils is zero. To solve this problem, we add (+1) to the longitudinal distance of adjacent foils and the equation for electric field distribution function in Fig. 2 changes into Eq. (6).

$$E=\frac{V}{\alpha L_x(\beta\frac{L_{p1}}{S_{p1}+1}+\gamma\frac{L_{p2}}{S_{p2}+1})} \tag{6}$$

The Eq. (6) is a mathematical model for proposed bushing of Fig. 2. In this mathematical model, the main effective parameters on bushing electric field are investigated.

Electric field minimum values

To minimize the numerical function given in Eq. (6), we should take the gradient of the equation and equal it to zero. Thus we will have Eq. (7).

$$\vec{\nabla}E=0 \tag{7}$$

In Eq. (7) the gradient function is defined as Eq. (8).

$$\vec{\nabla}E=\sum_{i=1}^{n}\frac{\partial E}{h_i\partial u_i}\hat{a}_{ui} \tag{8}$$

In Eq. (8) $\vec{\nabla}E$ is electric field gradient, h is metric coefficient, u is electric field function parameters and $\hat{a}_u$ are the unit vectors electric field. As there are six parameters in electric field function Eq. (8) changed into Eq. (9).

$$\vec{\nabla}E=\frac{\partial E}{h_1\partial u_1}\hat{a}_{u1}+\frac{\partial E}{h_2\partial u_2}\hat{a}_{u2}+\frac{\partial E}{h_3\partial u_3}\hat{a}_{u3}+\frac{\partial E}{h_4\partial u_4}\hat{a}_{u4}+\frac{\partial E}{h_5\partial u_5}\hat{a}_{u5}+\frac{\partial E}{h_6\partial u_6}\hat{a}_{u6} \tag{9}$$

Since we will solve Eq. (9) in Cartesian coordinate system, the metric coefficients equal one, Eq. (10).

$$h_1=h_2=h_3=h_4=h_5=h_6=1 \tag{10}$$

Therefore we have Eq. (11).

$$\vec{\nabla}E=\frac{\partial E}{\partial u_1}\hat{a}_{u1}+\frac{\partial E}{\partial u_2}\hat{a}_{u2}+\frac{\partial E}{\partial u_3}\hat{a}_{u3}+\frac{\partial E}{\partial u_4}\hat{a}_{u4}+\frac{\partial E}{\partial u_5}\hat{a}_{u5}+\frac{\partial E}{\partial u_6}\hat{a}_{u6} \tag{11}$$

We define the electric field parameters, Eq. (12), as follows:

$$\begin{aligned}u_1&=V\\u_2&=L_x\\u_3&=L_{p1}\\u_4&=S_{p1}\\u_5&=L_{p2}\\u_6&=S_{p2}\end{aligned} \tag{12}$$

Substituting Eq. (12) into (11), we have Eq. (13).

$$\vec{\nabla} E = \frac{\partial E}{\partial V}\hat{a}_V + \frac{\partial E}{\partial L_x}\hat{a}_{Lx} + \frac{\partial E}{\partial L_{p1}}\hat{a}_{Lp1} + \frac{\partial E}{\partial S_{p1}}\hat{a}_{Sp1} + \frac{\partial E}{\partial L_{p2}}\hat{a}_{Lp2} + \frac{\partial E}{\partial S_{p2}}\hat{a}_{Sp2} \tag{13}$$

Now, by partial differentiation in Eq. (6), we have Eq. (14).

$$\vec{\nabla} E = \frac{1}{\alpha L_X(\beta\frac{L_{p1}}{S_{p1}+1}+\gamma\frac{L_{p2}}{S_{p2}+1})}\hat{a}_V + \frac{-\alpha(\beta\frac{L_{p1}}{S_{p1}+1}+\gamma\frac{L_{p2}}{S_{p2}+1})V}{(\alpha L_X(\beta\frac{L_{p1}}{S_{p1}+1}+\gamma\frac{L_{p2}}{S_{p2}+1}))^2}\hat{a}_{Lx} + \frac{-\alpha L_X\beta\frac{1}{S_{p1}+1}V}{(\alpha L_X(\beta\frac{L_{p1}}{S_{p1}+1}+\gamma\frac{L_{p2}}{S_{p2}+1}))^2}\hat{a}_{Lp1} +$$
$$\frac{\alpha L_X\beta\frac{-L_{p1}}{(S_{p1}+1)^2}V}{(\alpha L_X(\beta\frac{L_{p1}}{S_{p1}+1}+\gamma\frac{L_{p2}}{S_{p2}+1}))^2}\hat{a}_{Sp1} + \frac{-\alpha L_X\gamma\frac{1}{S_{p2}+1}V}{(\alpha L_X(\beta\frac{L_{p1}}{S_{p1}+1}+\gamma\frac{L_{p2}}{S_{p2}+1}))^2}\hat{a}_{Lp2} + \frac{\alpha L_X\beta\frac{-L_{p2}}{(S_{p2}+1)^2}V}{(\alpha L_X(\beta\frac{L_{p1}}{S_{p1}+1}+\gamma\frac{L_{p2}}{S_{p2}+1}))^2}\hat{a}_{Sp2} \tag{14}$$

Regarding the fact that the unit vectors in Cartesian coordinates are as in Eq. (15), we have the Eq. (16).

$$\hat{a}_V = \hat{i}, \hat{a}_{Lx} = \hat{k}, \hat{a}_{Lp1} = \hat{k}, \hat{a}_{Sp1} = \hat{i}, \hat{a}_{Lp2} = \hat{k}, \hat{a}_{Sp2} = \hat{i} \tag{15}$$

$$\vec{\nabla} E = \frac{1}{\alpha L_X(\beta\frac{L_{p1}}{S_{p1}+1}+\gamma\frac{L_{p2}}{S_{p2}+1})}\hat{i} + \frac{-\alpha(\beta\frac{L_{p1}}{S_{p1}+1}+\gamma\frac{L_{p2}}{S_{p2}+1})V}{(\alpha L_X(\beta\frac{L_{p1}}{S_{p1}+1}+\gamma\frac{L_{p2}}{S_{p2}+1}))^2}\hat{k} + \frac{-\alpha L_X\beta\frac{1}{S_{p1}+1}V}{(\alpha L_X(\beta\frac{L_{p1}}{S_{p1}+1}+\gamma\frac{L_{p2}}{S_{p2}+1}))^2}\hat{k} +$$
$$\frac{\alpha L_X\beta\frac{-L_{p1}}{(S_{p1}+1)^2}V}{(\alpha L_X(\beta\frac{L_{p1}}{S_{p1}+1}+\gamma\frac{L_{p2}}{S_{p2}+1}))^2}\hat{i} + \frac{-\alpha L_X\gamma\frac{1}{S_{p2}+1}V}{(\alpha L_X(\beta\frac{L_{p1}}{S_{p1}+1}+\gamma\frac{L_{p2}}{S_{p2}+1}))^2}\hat{k} + \frac{\alpha L_X\beta\frac{-L_{p2}}{(S_{p2}+1)^2}V}{(\alpha L_X(\beta\frac{L_{p1}}{S_{p1}+1}+\gamma\frac{L_{p2}}{S_{p2}+1}))^2}\hat{i} \tag{16}$$

For electric gradient to be zero we have Eq. (17).

$$\begin{cases} \frac{1}{\alpha L_X(\beta\frac{L_{p1}}{S_{p1}+1}+\gamma\frac{L_{p2}}{Sp_2+1})} + \frac{\alpha L_X\beta\frac{-L_{p1}}{(S_{p1}+1)^2}V}{(\alpha L_X(\beta\frac{L_{p1}}{S_{p1}+1}+\gamma\frac{L_{p2}}{S_{p2}+1}))^2} + \frac{\alpha L_X\beta\frac{-L_{p2}}{(S_{p2}+1)^2}V}{(\alpha L_X(\beta\frac{L_{p1}}{S_{p1}+1}+\gamma\frac{L_{p2}}{S_{p2}+1}))^2} = 0 \\ \frac{-\alpha(\beta\frac{L_{p1}}{S_{p1}+1}+\gamma\frac{L_{p2}}{S_{p2}+1})V}{(\alpha L_X(\beta\frac{L_{p1}}{S_{p1}+1}+\gamma\frac{L_{p2}}{S_{p2}+1}))^2} + \frac{-\alpha L_X\beta\frac{1}{S_{p1}+1}V}{(\alpha L_X(\beta\frac{L_{p1}}{S_{p1}+1}+\gamma\frac{L_{p2}}{S_{p2}+1}))^2} + \frac{-\alpha L_X\gamma\frac{1}{S_{p2}+1}V}{(\alpha L_X(\beta\frac{L_{p1}}{S_{p1}+1}+\gamma\frac{L_{p2}}{S_{p2}+1}))^2} = 0 \end{cases} \tag{17}$$

The solution of Eq. (17) gives the condition for electric field minimum value in Eq. (6). According to the reference [7], the limits of α,β,γ are as Eq. (18).

$$\begin{cases} 4.5.10^{-6} < \alpha < 7.10^{-2} \\ 15 < \beta < 30 \\ 10 < \gamma < 25 \end{cases} \tag{18}$$

Where α is the longitudinal coefficient of the first aluminum coil and β,γ are the longitudinal coefficients of upper aluminum foil and lower aluminum coil respectively. Using MATLAB software estimator and simulation done in optometric section of MAXWELL software. The values of weighted coefficients α,β,γ are summarized as Table I.

Table I: Values of weighted coefficients

Weighted coefficients	Value
α	$5.46.10^{-6}$
β	20.92
γ	16.36

Regarding the condition for minimum electric field function in Eq. (17) and weighted coefficients α,β,γ in Table I. The values that make the function minimum are as follows:

$$L_x = 850mm, L_{p1} = 200mm, L_{p2} = 120mm, S_{p1} = 5mm, S_{p2} = 5mm$$

To investigate the correctness of this, we simulate the bushing using MAXWELL software. Using some points in simulation results and putting these points in electric field Eq. (6), we see that the results match (with maximum 1% error). This can be investigated using MATLAB software and by writing m-file.

Substitution of goal function coefficients from one side and the experiences of the manufacturing company from the other side have an important role for optimization. The weighted values of α,β,γ are shown in Table I. To determine the optimized points of effective parameters, Maxwell optometric tool is used which has the ability of optimization with the effect of each parameter and confirms the proposed model.

SIMULATION OF BUSHING ELECTRIC FIELDS

Condenser bushing meshed

The increase in the number of meshes in MAXWELL13 software increases precision or in other words decreases energy error. For this reason for simulation on condenser bushing we used 602 meshes which yielded good results. Condenser bushing meshing is shown in Fig. 3 [19].

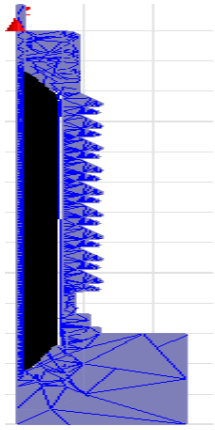

Fig. 3. Condenser bushing meshing

Simulation of condenser bushing

The simulation of condenser bushing, using structures in Fig. 4 and Fig. 5 is represented in this section. The first structure having coaxial cylindrical condensers configuration is shown in Fig. 4. And the condensers configuration in the structure 2 is shown in Fig. 5.

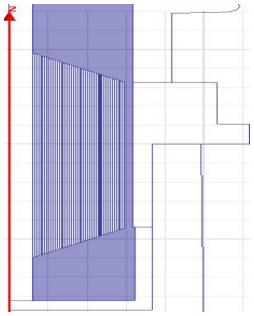

Fig. 4. First structure

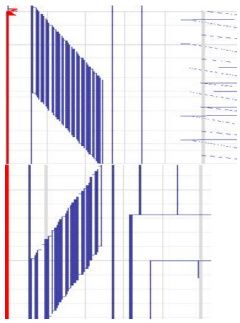

Fig. 5. Second structure

Simulation on condenser bushing is done and the results (due to symmetrical structure) are represented by two-dimensional structure for a 230kV bushing.

It should be mentioned that in 230kV condenser bushing, there is a need for condenser which has a significant effect on electric field and potential distribution in critical points. In methods used for construction of a condenser bushing, it should be taken into consideration that the structure of floating plates with coaxial cylindrical condenser configuration, has significant effect on uniformity and reduction of electrical tension on bushing flange metal part and on condenser bushing insulator abacuses [8-10],[20-24].

The simulation results of structures 1 and 2 for potential distribution and electric field are represented in Fig. 6 and Fig 7.

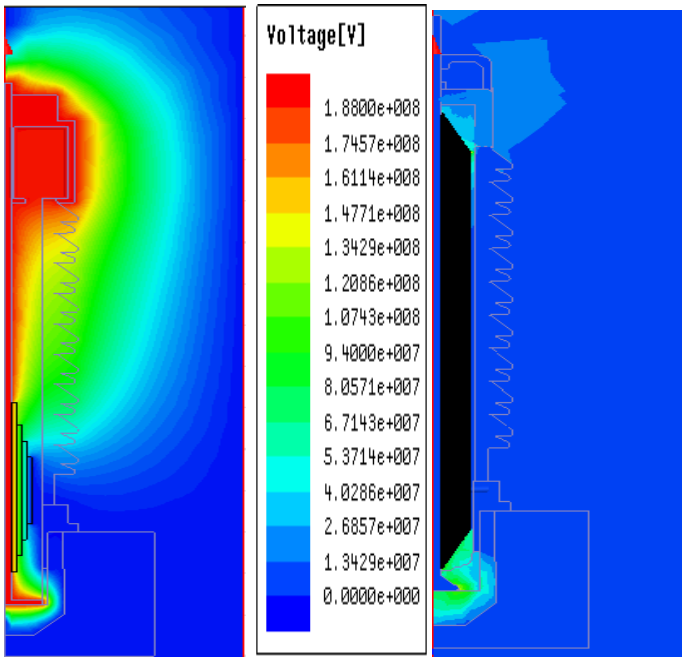

Fig. 6. Simulation results for voltage distribution in a 230kV bushing in structures 1and 2

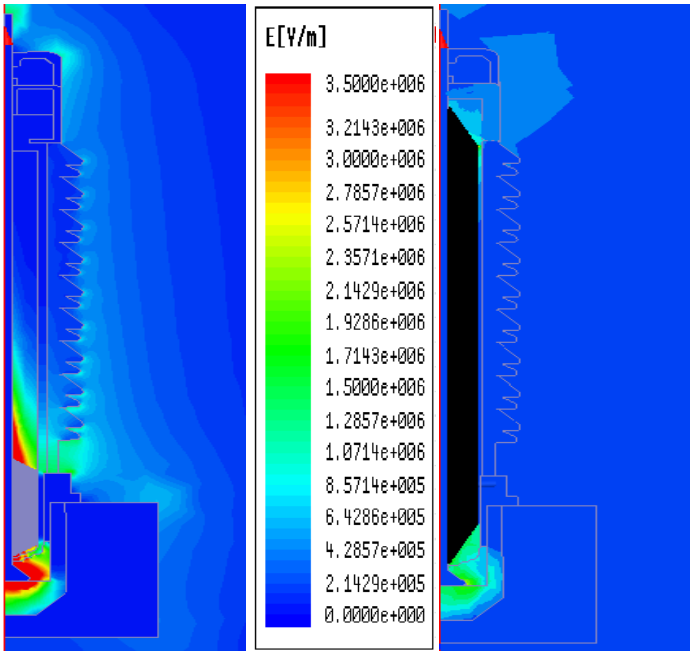

Fig. 7. Simulation results for electric field distribution in 230kV bushing in structures 1 and 2

Simulation Analysis

According to the simulation results, structure 1 makes electric field uniform on cylindrical condensers and has significant effect on reduction of electric field on metal sections of flange. Structure 2 significantly improves the reduction of electric field and potential field distribution in porcelain bushing structure, the results complies with calculations in next section.

In structure 2, there are significant results in bushing sensitive points for reduction of voltage and electric field concentration that prevent early erosion of porcelain insulators.

Voltage distribution on a condenser bushing with structure 1 is shown in Fig. 8. The zones in Fig. 8 are as follows:
Section 1 - Voltage distribution on the metal section of aluminum flange that is in the range of 0 to 37kV
Section 2 - Voltage distribution on porcelain insulator that ranges between 37kV to 157kV
Section 3 - Voltage distribution on the upper part of condenser bushing ranging between 157kV to 188kV

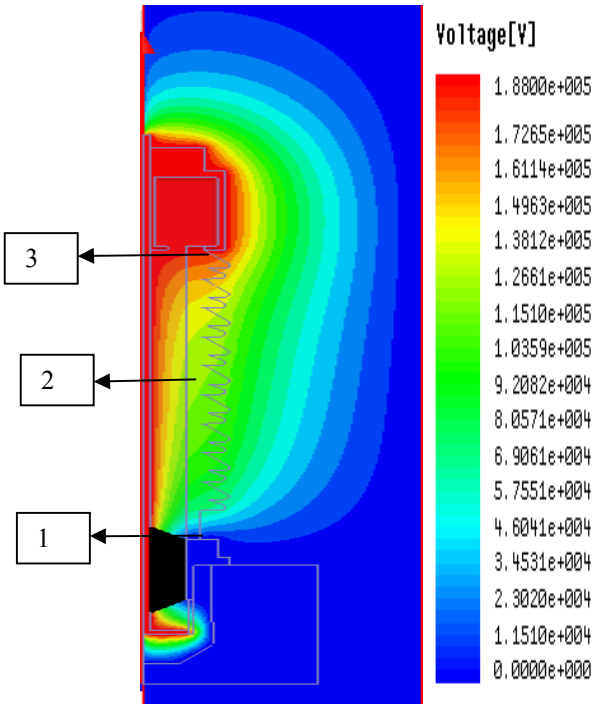

Fig. 8. Voltage distribution on insulator abacuses of conventional bushing (structure 1)

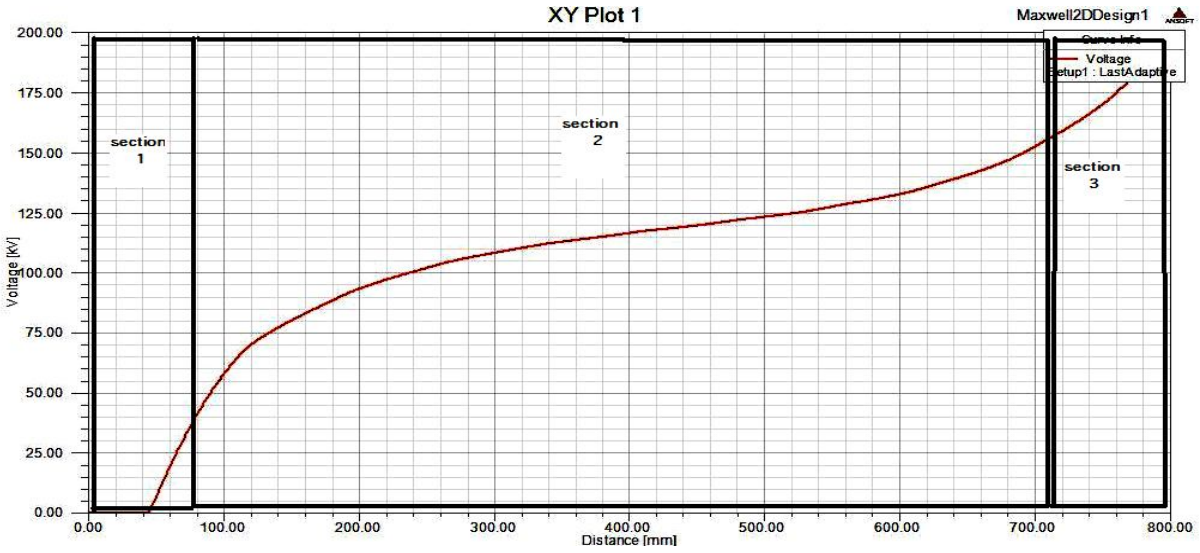

Fig. 9. Voltage distribution on abacus of insulator bushing in z-axis in structure 1

Voltage distribution on condenser bushing with structure 2 is shown in Fig. 10. In Fig. 10 we have the following zones:

Section 1 - Shows voltage distribution on metal section of aluminum flange. The voltage range is between 0 to 2kV

Section 2 - Shows voltage distribution on porcelain insulator. The voltage ranges between 2kV to 60kV

Section 3 - Shows voltage distribution on the upper section of condenser bushing. The voltage ranges between 60kV to 188kV.

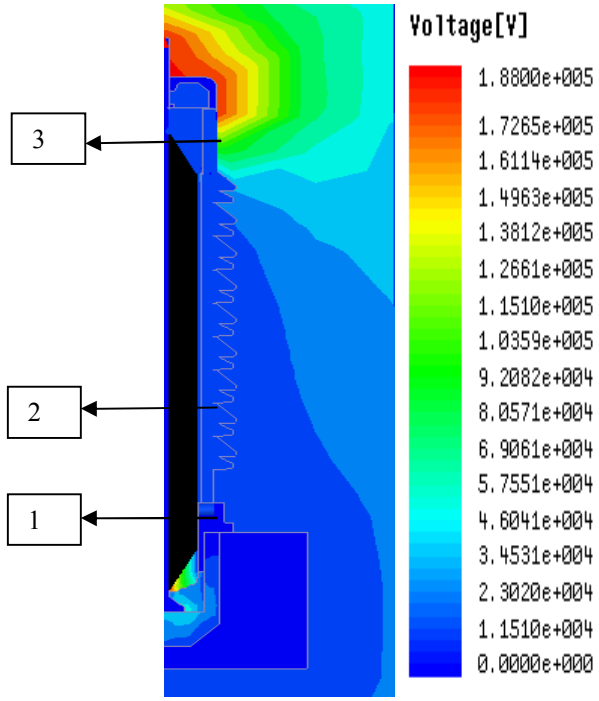

Fig. 10. Voltage distribution on bushing insulator abacus with structure 2

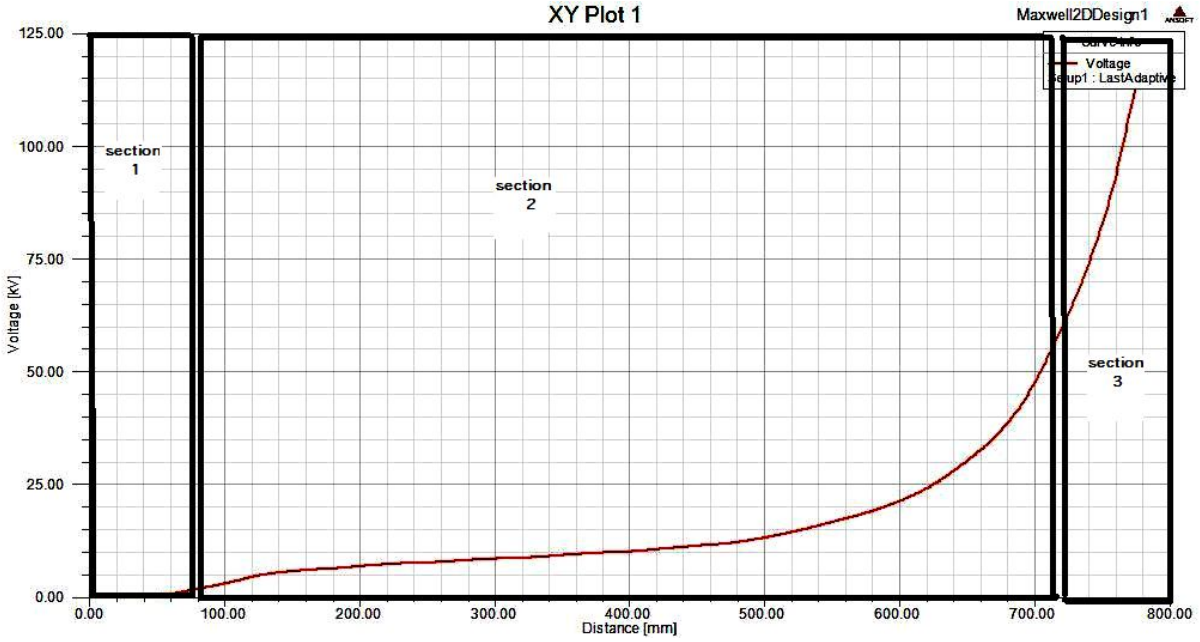

Fig. 11. Voltage distribution curve in z-axis direction in structure 2

By comparison of the two condenser structures, we can notice the advantages of structure 2 over structure 1. Since the reduction of voltage concentration in zones 1, 2, 3 are 35kV, 97kV, 97kV respectively. The electrical tension reduces which lengthens the bushing life-time.

The electric field distribution on condenser bushing of structure 1 is shown in Fig. 12. According to Fig. 12 we have:

Section 1 - Shows the electric field distribution on metal section of aluminum flange. The maximum value for this section is 12kV/cm

Section 2 - Shows the electric field distribution on the porcelain insulator. The maximum value for this section is 7.5kV/cm

Section 3 - Shows the electric field on upper section of condenser bushing. The maximum value for this section is 3.6kV/cm

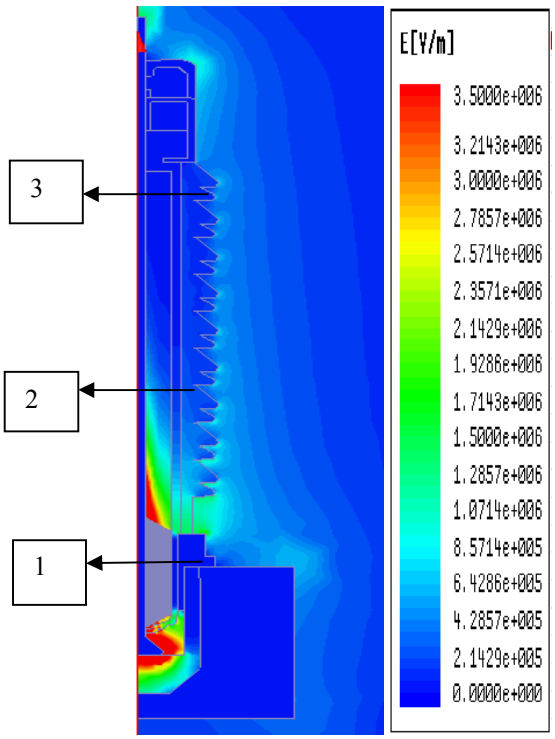

Fig. 12. Electric field intensity in bushing with structure 1

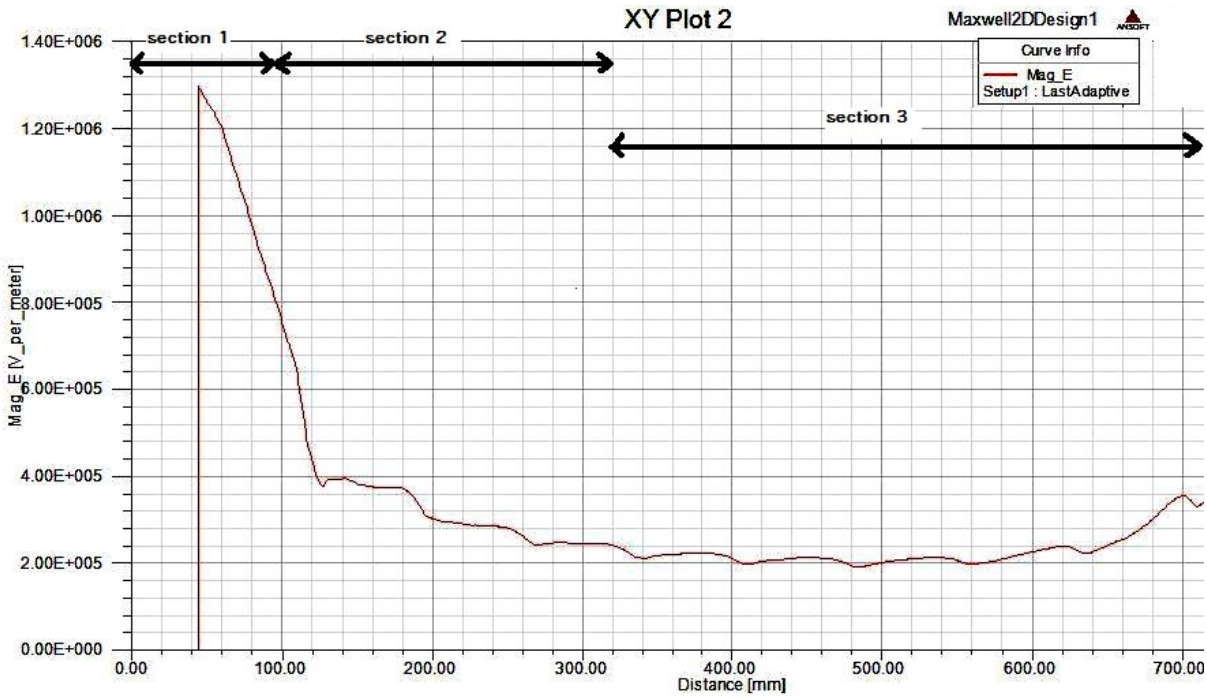

Fig. 13. Electric field distribution curve in z-axis direction in structure 1

The electric field distribution on condenser bushing of structure 2 is shown in Fig. 14. According to the Fig. 14 we have:

Section 1 - Shows electric field distribution on metal section of aluminum flange. The maximum value is 0.2kV/cm

Section 2 - Shows the electric field distribution on porcelain insulator. The maximum value in this section is 0.4kV/cm

Section 3 - Shows the electric field distribution on the upper section of condenser bushing. The maximum value for this section is 2.9kV/cm

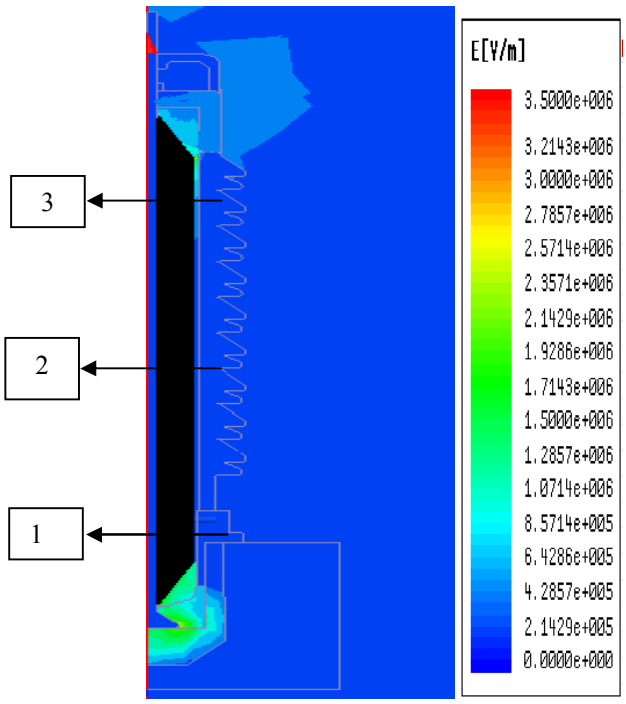

Fig. 14. Bushing electric field intensity with structure 2

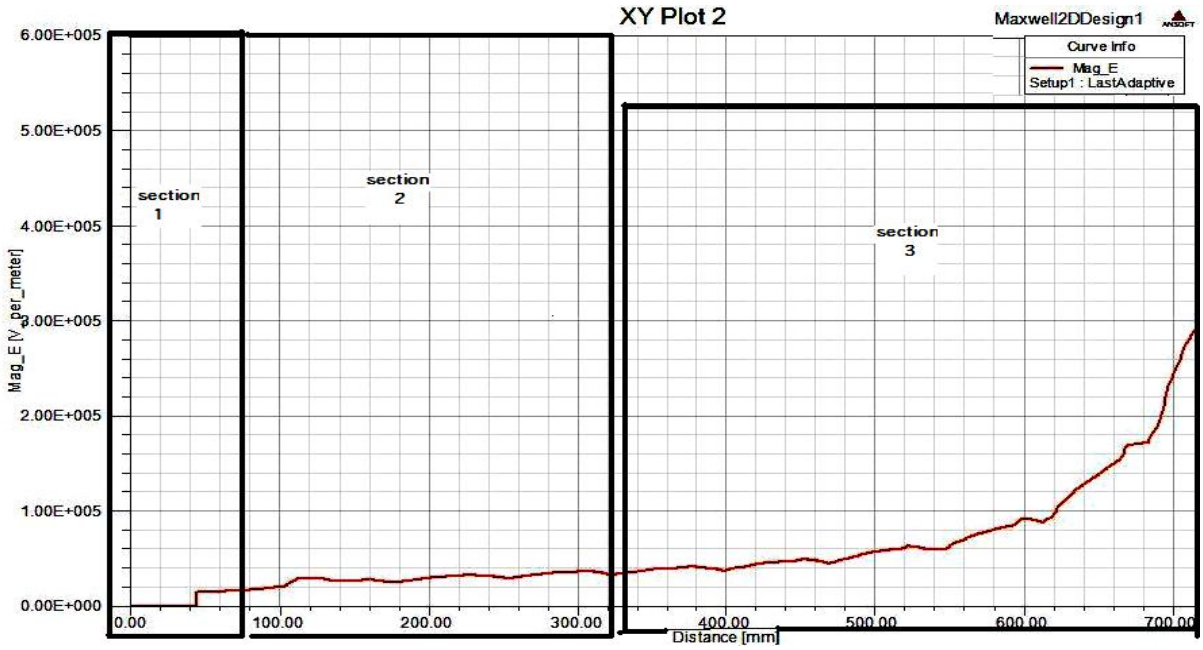

Fig. 15. Electric field distribution curve in z-axis direction in structure 2

Regarding the values from electric field intensity distribution, the condenser structure 2 shows improvement compared to condenser structure 1. Reduction of electric field intensity in sections 1,2,3 are 11.8kV/cm, 7.1kV/cm and 0.7kV/cm respectively. The electric field intensity distribution plot on condenser bushing with both structures is shown in Fig. 16 and Fig. 17.

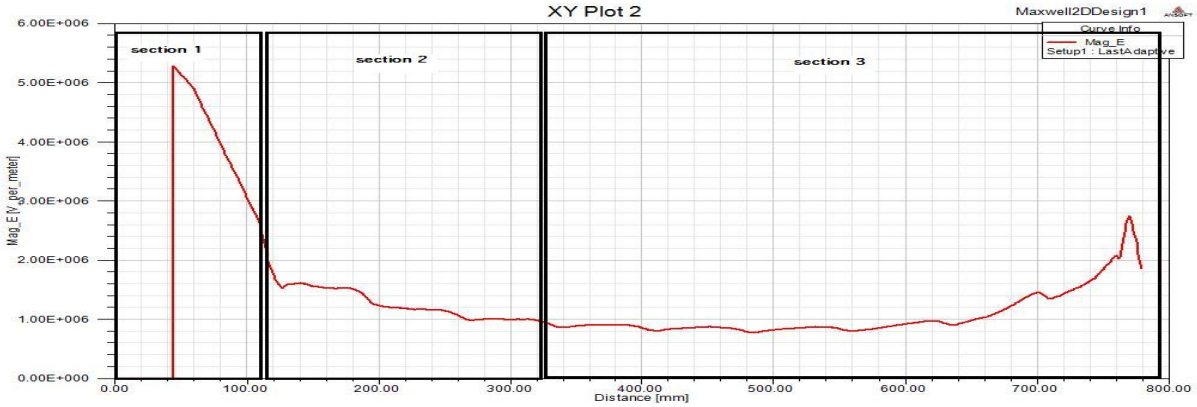

Fig. 16. Electric field intensity plot in z-axis direction for structure 1

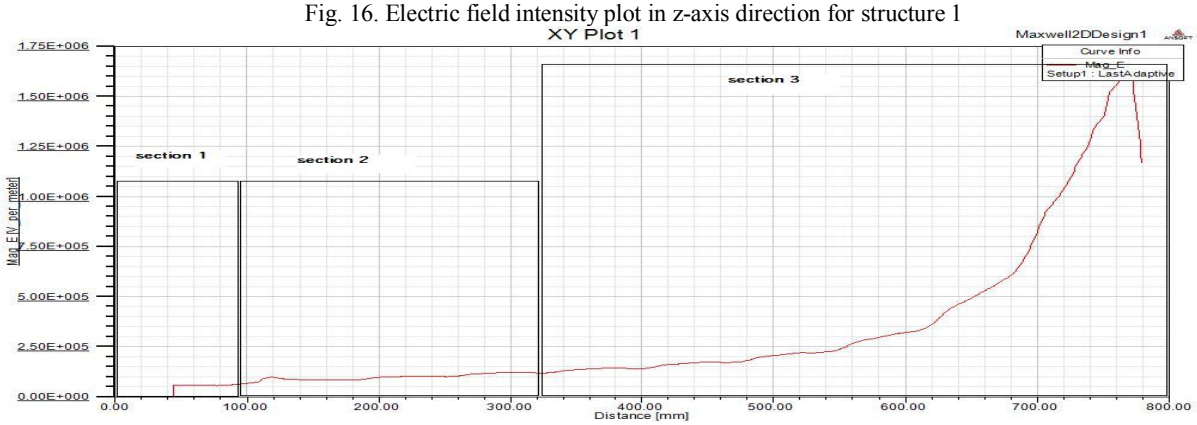

Fig. 17. Electric field intensity plot in z-axis direction for structure 2

In section 1and structure 2 are completely superior to structure 1. In the section2, the maximum value of electric field on porcelain insulators of structures 1 and 2 are 5.4kV/cm and 40kV/cm respectively. According to Table II, the break down voltage in structure 1 is 30kV/cm. The tension value is above the permitted value which causes insulation break down and decreases the insulator life time.

Table II: The electrical characteristics of insulating material used in 230kV bushing simulation

Material name	**ε (insulation number)**	**Electric field break down (electric strength) H$\frac{KV}{cm}$**
Impregnated paper	3.2	**40**
Oil	2.2-2.45 (depends on temperature)	**20**
Aluminum foil	1 (no load condition)	**-**
Resin	4.2	**30**
Air	1	**17**
Porcelain	5.7	**30**

OPTIMIZATION OF CONDENSER BUSHING

For parametric solution and optimization of bushing model, we should first define the variables that exist in the bushing active part. The variables are in Table III.

Table III: Values of variable parameters of condenser bushing

Variable name	s_{p_2}	s_{p_1}	l_{p_2}	l_{p_1}	l_x
Normal size (mm)	5	7	115	260	800

According to Table IV, we define the range of variable parameters. It should be noted that these parameters not to be defined out of acceptable range [7].

Table IV: The range of variable parameters

Variable name	s_{p_2}	s_{p_1}	l_{p_2}	l_{p_1}	l_x
Normal value (mm)	5	7	115	260	800
Simulation range (mm)	2.5-7.5	3.5-10.5	57-172	130-390	500-1500

Parametric optimization

In this section by entering variables and choosing different cases we can observe voltage and electric field distribution for all conditions. In Fig. 18, the voltage behavior is observed for all iterations.

Fig. 19 also shows the electric field intensity along the conductor under voltage length up to aluminum flange.

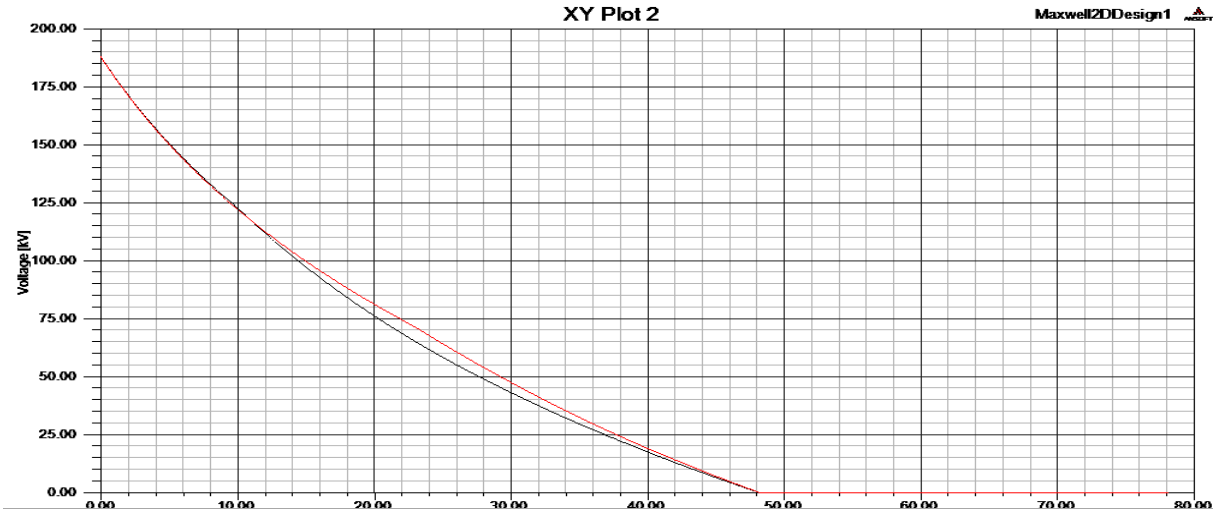

Fig. 18. Minimum and maximum voltage drop in each condenser layer versus the radius of layers

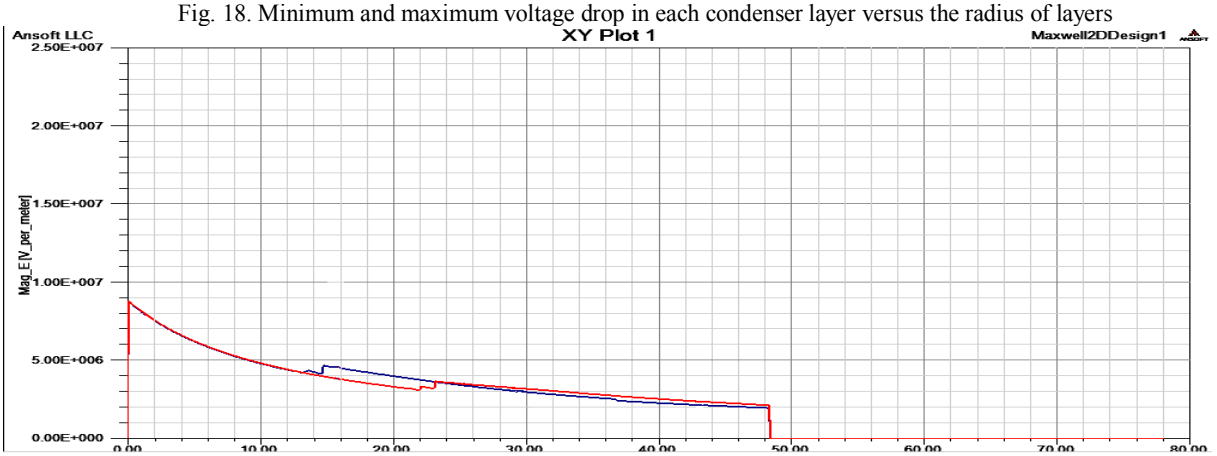

Fig. 19. Minimum and maximum electric field intensity plot for different cases in structure 2

Optimization of dimensions

Optimization of condenser bushing was done according to variation range in Lx, Lp_1, Lp_2, Sp_1, Sp_2. The maximum output electric field intensity in all cases is as Fig. 20.

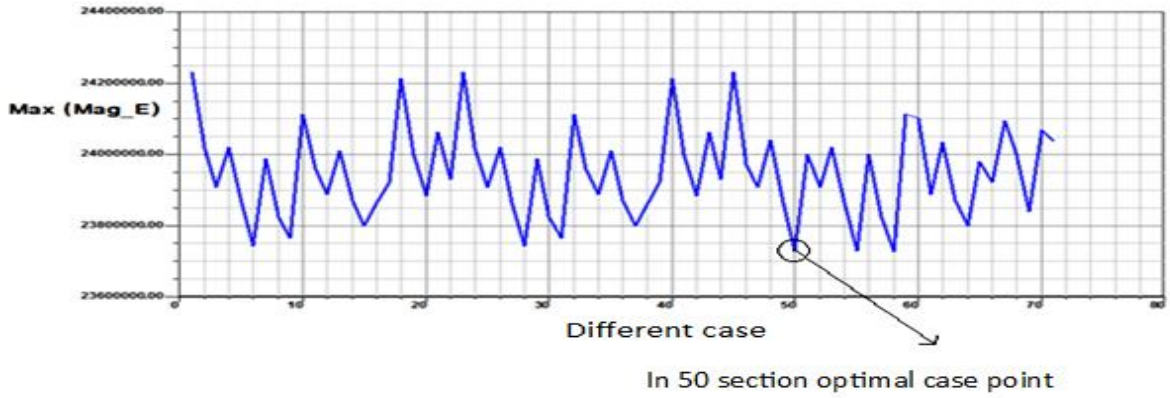

Fig. 20. Maximum output for electric field intensity based on variations

In Fig. 20, case 50 is the least minimum point for electric field intensity. The optimized values have also been resulted for case 50 in Table V.

Table V: Optimized values for condenser bushing structure to minimize electric field intensity

Maximum electric field intensity (V/m)	Sp_2(mm)	Sp_1(mm)	L_X(mm)	L_{P2}(mm)	L_{P1}(mm)	Case
$2.3729X10^7$	5	5	850	120	200	50

CONCLUSION

In this paper, the optimized design of a 230kV condenser bushing from the electrical field intensity and voltage distribution aspects and over two condenser structures has been investigated. Optimization of dimensions of condensers and calculation of weight coefficients to minimize electric field are the main goals of this paper to achieve the optimized geometric shape of high voltage bushing to reduce electric field intensity and voltage distribution in aluminum flange section and porcelain insulator and upper section of bushing. Variation of dimensions of condensers along the bushing reduced the electric field intensity and made it uniform in the active section.

REFERENCES

1. Hashemighiri, Farjahebrahim, Seifialireza, "Optimization of condenser bushing using electrostatic simulation", International Power System Conference (PSC), 09-F-HVS-0109, (2009).
2. Alireza Setayeshmehr, Alireza Akbari, Hossein Borsi and Ernst Gockenbach, "On-line Monitoring and Diagnoses of Power Transformer Bushings", IEEE Conference, Germany, (2006).
3. Mahmood Hadighi, Akbari Asghar, Hasibbabai Faramarz,"Optimization of a condenser sensor to receive partial discharge signals in power transformers", International Power System Conference (PSC), (2008).
4. J.W. Choi, J.H. Choi, H.J. Kim, J.W. Cho, S.H. Kim, "A study on designing the electrical insulation of condenser – type terminations for 154 kV class HTS cables", Elsevier journal, pp. 1707-1711, (2009).
5. S. Zhang, "Evaluation of Thermal Transient and Overload Capability of High-Voltage Bushings with ATP", IEEE Transaction on Power Delivery, Vol. 24, no. 3, USA, pp. 1295-1301, July (2009).
6. Mohamad R. Hesamzadeh, Nasser Hosseinzadeh and Peter Wolfs, "An Advanced Optimal Approach for High Voltage ACBushing Design", IEEE Transaction on Dielectrics and Electrical Insulation, Vol. 15, no. 2, pp. 461-466, April (2008).
7. Fattahi Farrokh, "Fundamentals of high voltage engineering and electrical insulation", hydro and power higher educational-vocational institute, 1st edition, 2009.
8. R. Arora, W. Mosch, "High voltage Engineering", first edition, 1995, reprint 2004.
9. Hoshmand Rahmatollah, Saghafi Mehdi, "Insulation and High Voltage", Ahwaz, Shahid Chamran University press, 2003.
10. D.S. Kwag, H.G. Cheon, J.H. Choi, S.H. Kim, "Research on the electrical insulation design of a bushing for a 154 kV class HTS transformer", Elsevier journal, pp. 1213-1217, (2007).
11. Morteza Mozaffari, "Simulation of high voltage sections of 230kV optical voltage transformers using FLUX software", International Power System Conference (PSC), 09-F-HVS-0109, (2009).
12. R S. Monga, R. S. Gorurt, P. Hansen and W. Massey, "Design Optimization of High Voltage Bushing Using Electric Field Computations", IEEE Conference, Arizona, pp. 1217-1224, (2006).
13. Keith P. Ellis, "Bushing for Power Transformers", Trench Limited.
14. P. Kitak, J. Pihler and I. Ticar, "Optimization algorithm for the design of bushing for indoor SF6 switchgear applications", IEEE Conference, SLOVENIA, pp. 691-696, (2005).
15. A. Filiatrault, M. Eeri and H. Matt, "Experimental Seismic Response of High Voltage Transformer Bushing Systems", Earthquake Spectra, Vol. 21, IEEE Transaction, pp. 1009-1025, Jan. (2005).
16. S. Zhang, "Analysis of Some Measurement Issues in Bushing Power Factor Tests in the Field", IEEE Conference, Australia, (2008).
17. Resin impregnated paper bushings, product information, ABB Power Technology products, D. Meeker, Components, www.abb.com
18. Platek, R. Sekula, R. Platek and B. Lewandowski, "Fluid Influence on Dynamic Characteristics of Transformer Bushing System using Fluid Structure Interaction (FSI) Approach", IEEE Transactions on Dielectrics and Electrical Insulation, Vol. 17, No. 2, pp. 408-416, April (2010).
19. Help Maxwell13
20. H.J. Lingal, H.L. Cole, T.R. Watts, "Oil Impregnated Paper High Voltage Condenser Bushings For Circuit Breakers and Transformers", IEEE Conference, New York, pp. 269-275, (2006).
21. Selahattin Ersoy and M. Ali Saadeghvaziri, "Seismic Response of Transformer-Bushing Systems", IEEE Transactions on Power Delivery, Vol. 19, no. 1, pp. 131-137, Jan. (2004).
22. D. Meeker, "Finite element method magnetic", Version 4.2, User's manual, pp. 50-51, 149-150, March (2007).
23. J. Rocks, N. Koch, R. Platek and T. Nowak, "Seismic Response of RIP transformer bushing", Insulator News & Market Report (INMR), World Congress on insulators, arresters and bushings, IEEE Conference, Brazil, (2007).
24. Transformer Oil handbook, NYNAS, www.nynas.com/naphthenics